Supplementary Table 1. Number of water molecules forming H-bonds with lipids revealed by MD simulations.

	Lipid	Number of water molecules
11C Wild-type	PtdSer	0.5
	PtdCho	3.8
	PtdEtn	2.7
11C Q79E	PtdSer	3.7
	PtdCho	3.0
	PtdEtn	0.9
11C Q79A	PtdSer	0.8
	PtdCho	3.0
	PtdEtn	2.2
8A1 Wild-type	PtdSer	3.5
	PtdCho	5.8
8A1 Q88E	PtdSer	8.6
	PtdCho	5.6
8A1 Q88A	PtdSer	5.8
	PtdCho	1.7

Supplementary Table 2. Primers

Primers for mouse genotyping

ATP11A^{flox}	CGTGCAATCCATCTTGTTCAAT	GAATGAGATCAGTCAGAAAGGACAG
ATP11A^{Q84E}	ATCATGGAAGCAGCCCTAAG	TGAGTCAAGGCAGAGAGCAA
CAG-Cre	CGCGATTATCTTCTATATCTTCAGG	AGGTCGTTATTCGGATCATCAGCTA

Primers for recombinant PCR for mutagenesis of human ATP11A, ATP8A2 and ATP11C

	Common forward primer	complementary mutagenizing primers		common reverse primer
hATP11A				
Q84A	GGCTTAATTAAGGAGGAGCCATG	ATATTTCTGGTGGCCTTGATTATTG	CAATAATCAAGGCCACCAGAAATAT	GCCGAATTCGAAACTCAGGCTGC
Q84N		ATATTTCTGGTGAACTTGATTATTG	CAATAATCAAGTTCACCAGAAATAT	
Q84D		ATATTTCTGGTGGACTTGATTATTG	CAATAATCAAGTCCACCAGAAATAT	
hATP8A2				
Q107E	CTAGTTTAATTAAGCCACCATGCTG	CGCCCTGCTGGAGCAGATCCCCGAC	GTCGGGGATCTGCTCCAGCAGGGCG	GGTCACGCCGGCGATAGAGCACTTC
Q107A		GCCCTGCTGGCGCAGATCCCCGAC	GTCGGGGATCTGCGCCAGCAGGGC	
hATP11C				
Q79E	AGTTTAATTAAGCCACCATGTTCAG	CTTCCTGGTGGAAGTGACCGTGGAC	GTCCACGGTCACTTCCACCAGGAAG	GGTGCTGCCATCGATGATCAGTCCG
Q79A		CTTCCTGGTGGCAGTGACCGTGGAC	GTCCACGGTCACTGCCACCAGGAAG	

*Restriction enzyme recognition sites and mutated residues are singly- and doubly underlined, respectively.

Primers for RT-PCR

mouse *SGMS1*	ACTGGTCACCCAAGAAGGTG	TCTAAGAGTCGCTGCCCATT
mouse *36B4*	GCTCCAAGCAGATGCAGCA	CCGGATGTGAGGCAGCAG
human ATP11A	GCTGCTGCAGGCTGCCAAAG	GTCTCTGGTCAGGCTCCCGC
human 36B4	GCTCCAAGCAGATGCAGCA	CCGGATATGAGGCAGCAG

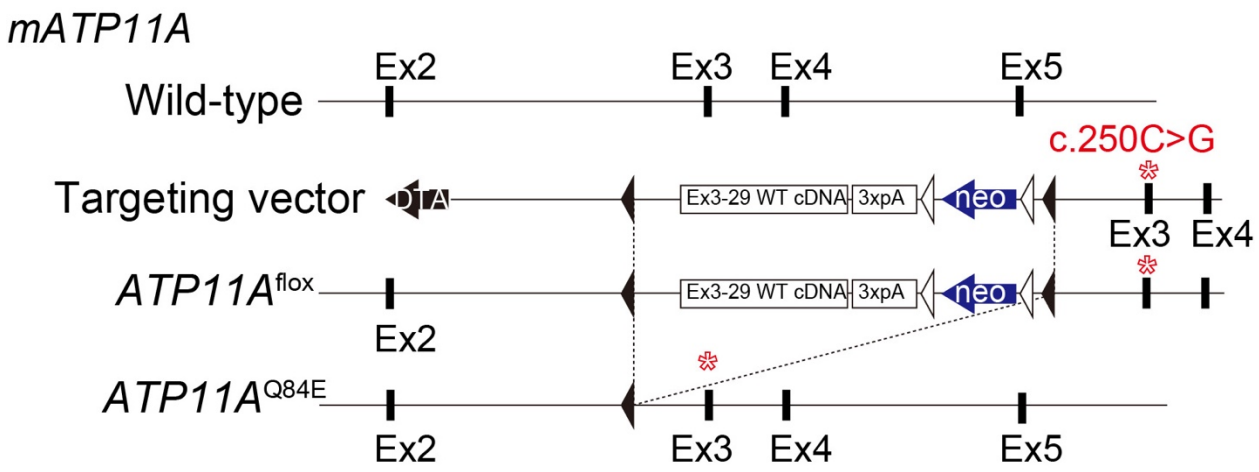

Supplementary Figure 1. Gene targeting strategy to produce mice carrying the Q84E mutation in the *ATP11A* gene. cDNA for exons 3-29 of the m*ATP11A* gene and three SV40 poly(A) addition signals (3×pA) were inserted into intron 2, followed by *PGK-neo* (neo). Exons are in numbered black boxes. The red asterisk indicates the point mutation, c.250C>G. The recognition sites for FRT (flippase recognition target) and LoxP (locus of X-overP1) are indicated by white and black triangles. The black arrow shows DNA for the diphtheria toxin A fragment (DTA).

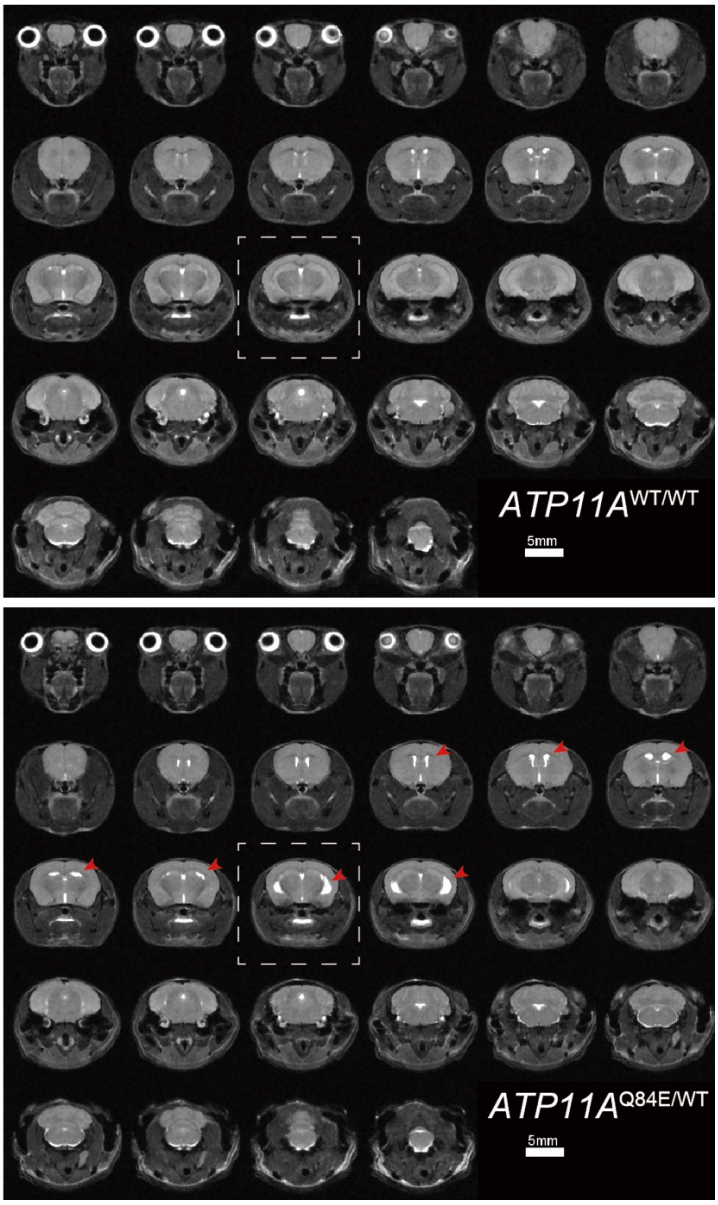

Supplementary Figure 2. MRI of the mouse brain. T2-weighted MRI scans of 11-week-old *ATP11A*$^{WT/WT}$ and *ATP11A*$^{Q84E/WT}$ female mouse brains are shown. The images indicated by the dashed boxes are in Figure 3E. Red arrowheads indicate dilation of the lateral ventricle in the mutant mouse. Scale bar, 5 mm.

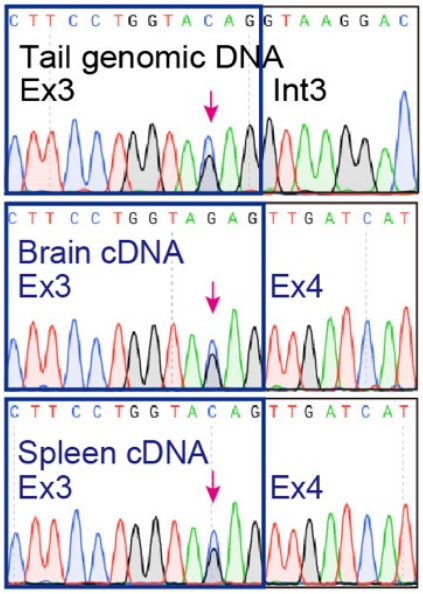

Supplementary Figure 3. Expression of mutant mRNA in the *ATP11A*$^{Q84E/WT}$ mouse. DNA was prepared from the tail of an *ATP11A*$^{Q84E/WT}$ mouse, and the locus containing the mutation was analyzed by Sanger sequencing (Top panel). In the middle and lower panels, RNA was prepared from the brain and spleen of the *ATP11A*$^{Q84E/WT}$ mouse and reverse-transcribed. The region of the mATP11A gene containing the Q84E mutation was subjected to Sanger sequencing. The heterozygous mutation is indicated by a red arrow. In tail DNA, the sequence of exon 3 (Ex3) continues to the sequence of intron 3 (Int3), while the exon 3 is joined to exon 4 in cDNA.

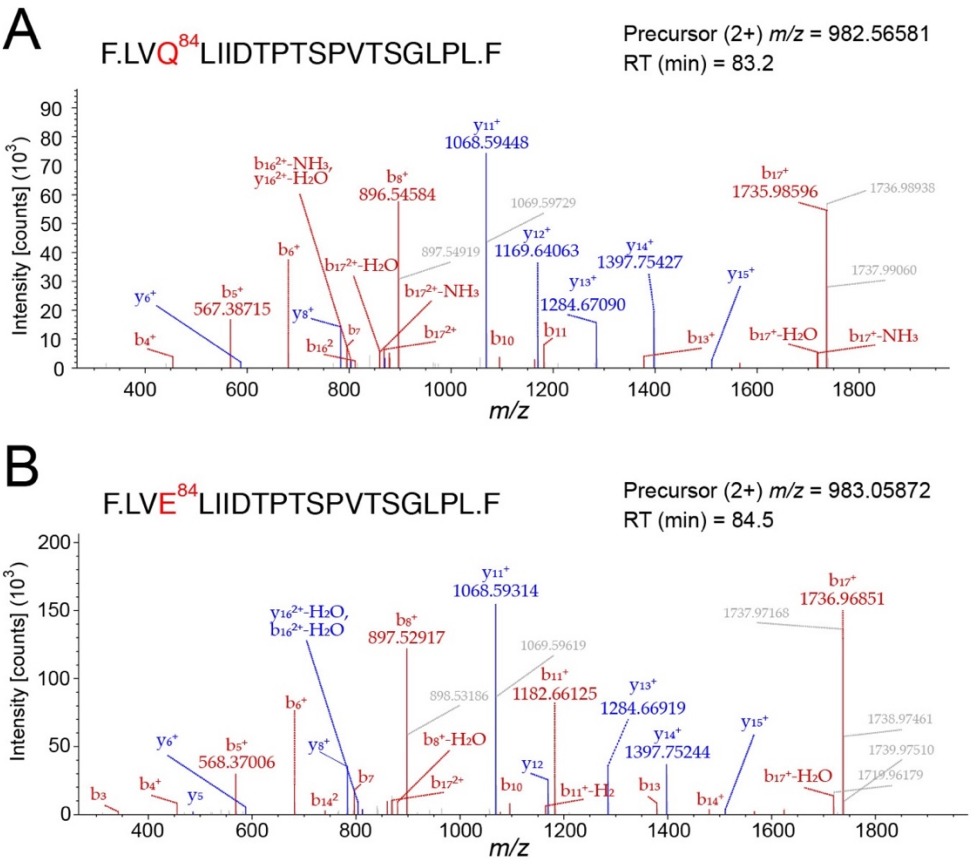

Supplementary Figure 4. LC-MS/MS analysis of Q84- or E84-containing peptides. Cell lysates were prepared from DKO cells expressing the GFP-tagged WT (**A**) or Q84E mutant of hATP11A (**B**) and subjected to immunoprecipitation with anti-GFP nanobody. Immunoprecipitates were digested with chymotrypsin and analyzed by the data-dependent LC-MS/MS. Fragmented peptide ions containing Q84 (b_5^+-567.38715; b_8^+, 896.54584; b_{17}^+-1735.98596) or E84 (b_5^+-568.37006; b_8^+, 897.52917; b_{17}^+-1736.96851) of ATP11A were identified from the MS/MS spectra of *m/z* 982.56581 and 983.05872 ions.

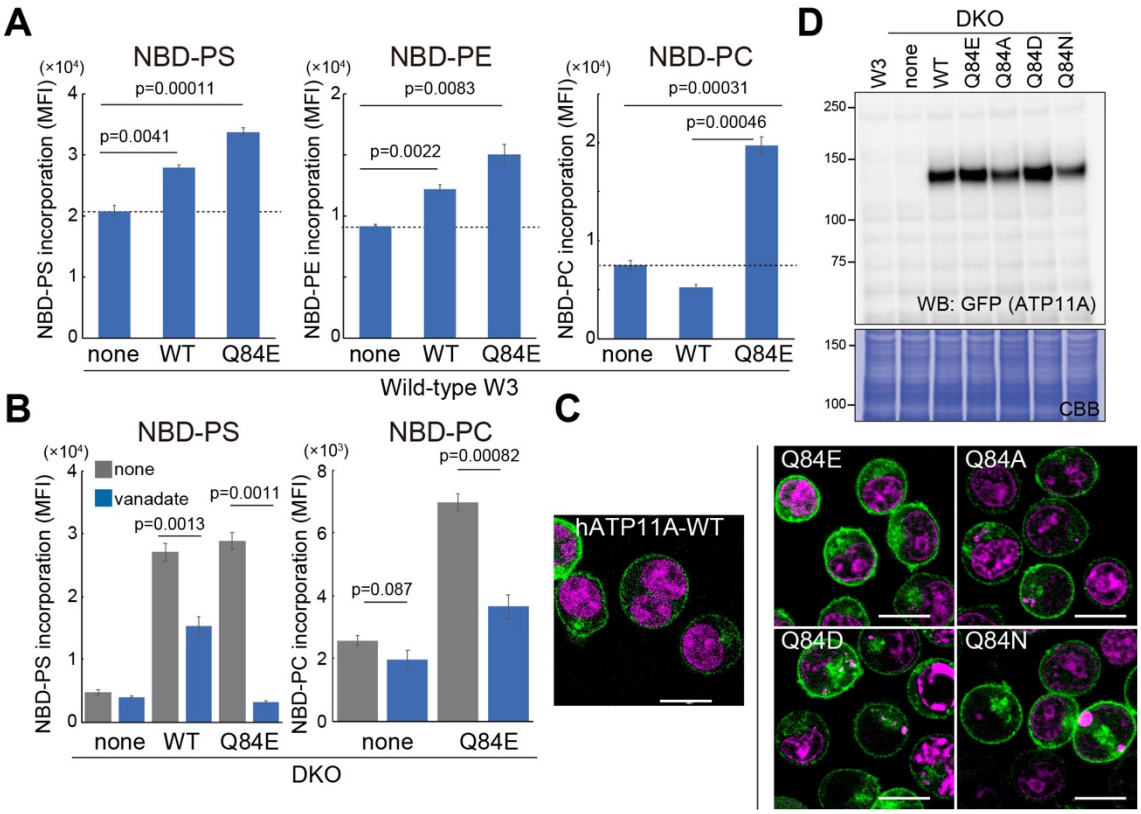

Supplementary Figure 5. Expression, localization, and flippase activity of *ATP11A* mutants. (A and **B)** Wild type W3 (**A**) or DKO (**B**) cells were transformed with GFP-tagged WT or Q84E mutant hATP11A together with CDC50A, incubated at 20ºC with 500 nM NBD-PS for 3 min, 500 nM NBD-PE for 20 min, or 250 nM NBD-PC for 15 min in the presence/or absence of 10 mM vanadate (**B**), and analyzed by flow cytometry. Experiments were performed three times, and the average MFI value was plotted with S.D. (bar). (**C** and **D**) DKO cells were transformed with GFP-tagged WT or Q84A, Q84E, Q84D, or Q84N mutant hATP11A together with CDC50A, and observed by confocal fluorescence microscopy after staining with DRAQ5 (**C**) or analyzed by Western blotting with anti-GFP Ab (**D**). The membrane used for western blotting was also stained with CBB (bottom). Green, GFP; Magenta, DRAQ5 (nucleus). Scale bar, 10 μm.

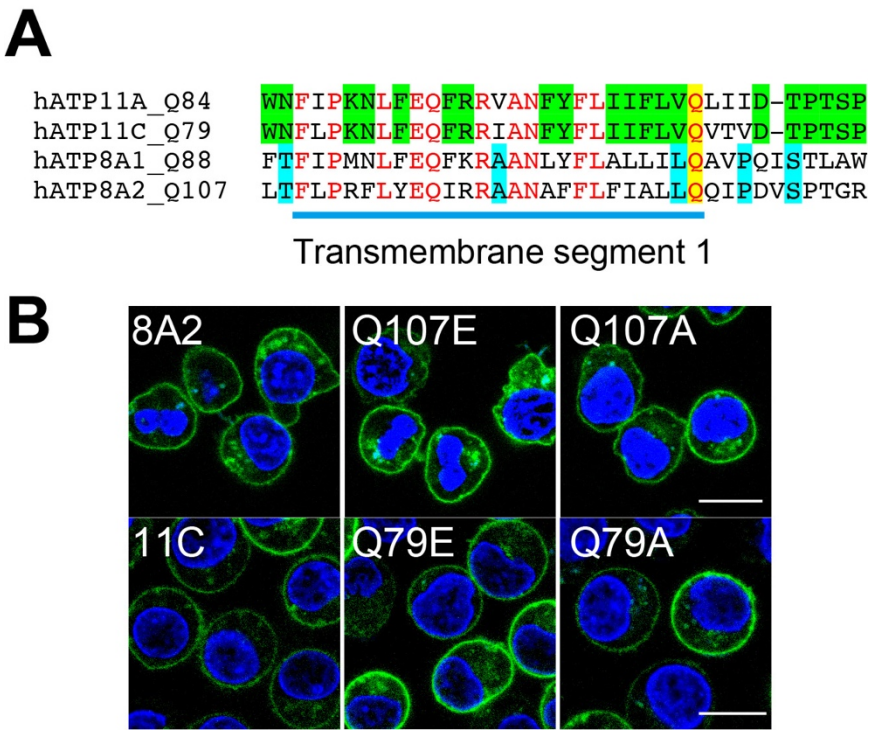

Supplementary Figure 6. Expression and localization of ATP11C and ATP8A2 mutants. (**A**) Amino acid sequences around the first transmembrane region of human ATP11A, 11C, 8A1, and 8A2. "Q"s corresponding to Q84 in ATP11A are highlighted by yellow. (**B**) DKO cells expressing the indicated GFP-tagged WT (8A2 and 11C) or mutant of hATP8A2 (Q107E and Q107A) or hATP11C (Q79E and Q79A) were observed by confocal microscopy. Green, GFP; Blue, nucleus.

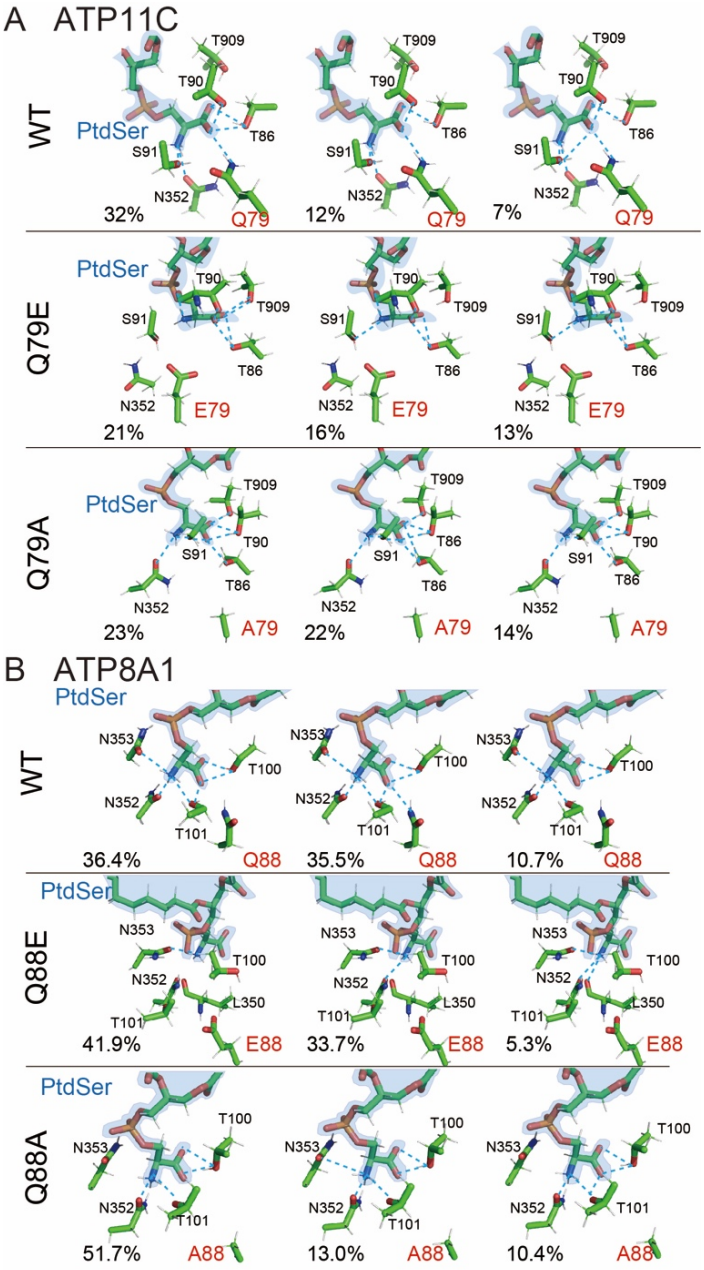

Supplementary Figure 7. H-bond patterns in ATP11C and ATP8A1 with PtdSer. Three major H-bond patterns with PtdSer in the wild-type (WT) and indicated mutant ATP11C (**A**) and ATP8A1 (**B**) are shown. H-bonds are shown in dashed lines. The percentages of the respective patterns are indicated. PtdSer is enclosed by a blue-shadowed area.

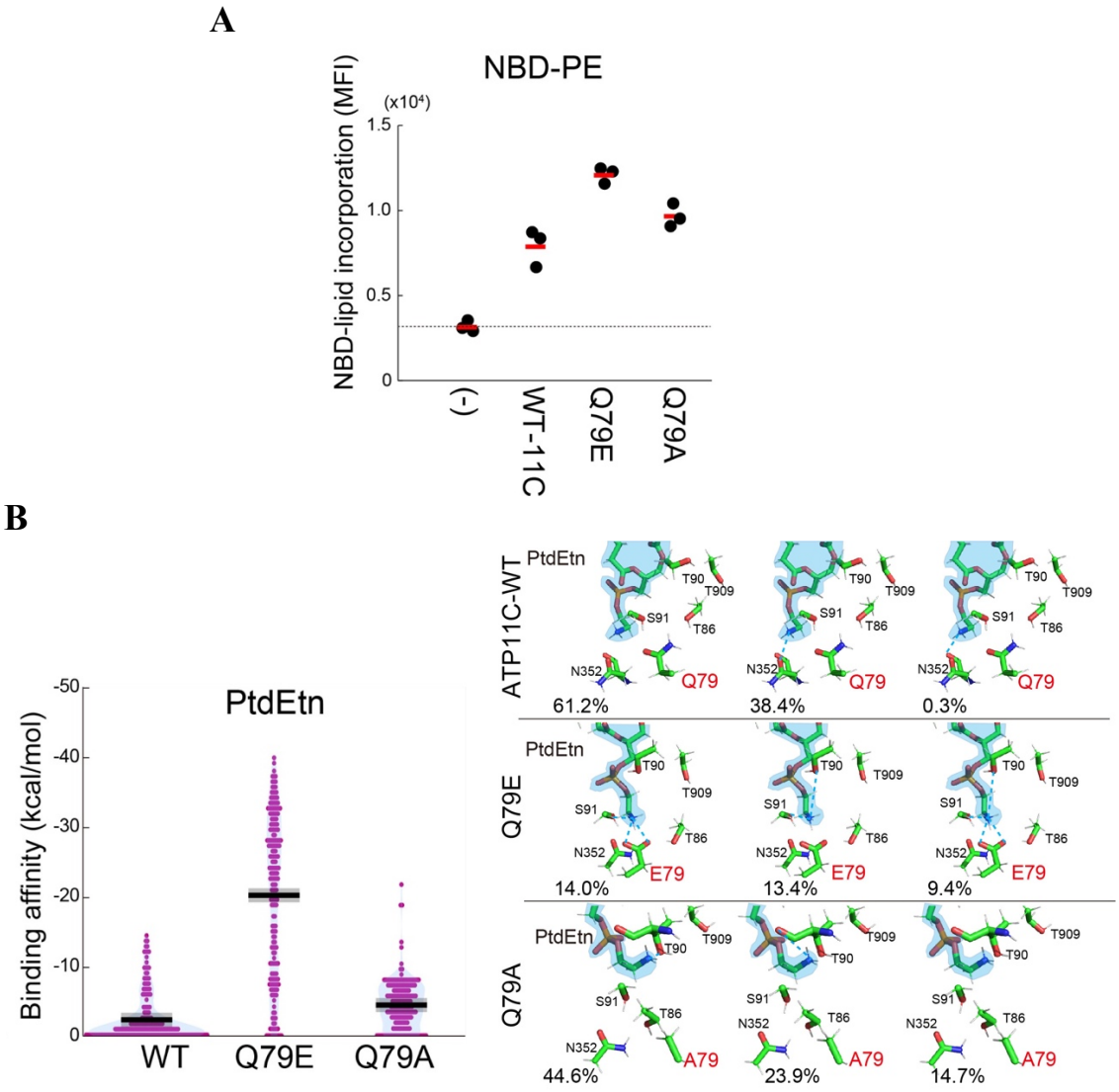

Supplementary Figure 8. Flipping activity and binding affinity of hATP11C for PtdEtn. (**A**) DKO, and its transformants expressing GFP-tagged wild-type (WT)- or mutant hATP11C were incubated with 500 nM NBD-PE at 20°C for 20 min and then analyzed by flow cytometry. MFI is plotted with mean values (Bars). (**B**) The binding energies of PtdEtn to WT-, Q79E-, and Q79A-hATP11C were calculated by an MD simulation analysis (n=200 structures). Bars indicate mean values. On the right, three major H-bond patterns with PtdEtn in the wild-type and indicated mutant ATP11C are shown. H-bonds are in dashed lines. The percentages of the respective patterns are indicated. PtdEtn is enclosed by a blue-shadowed area.

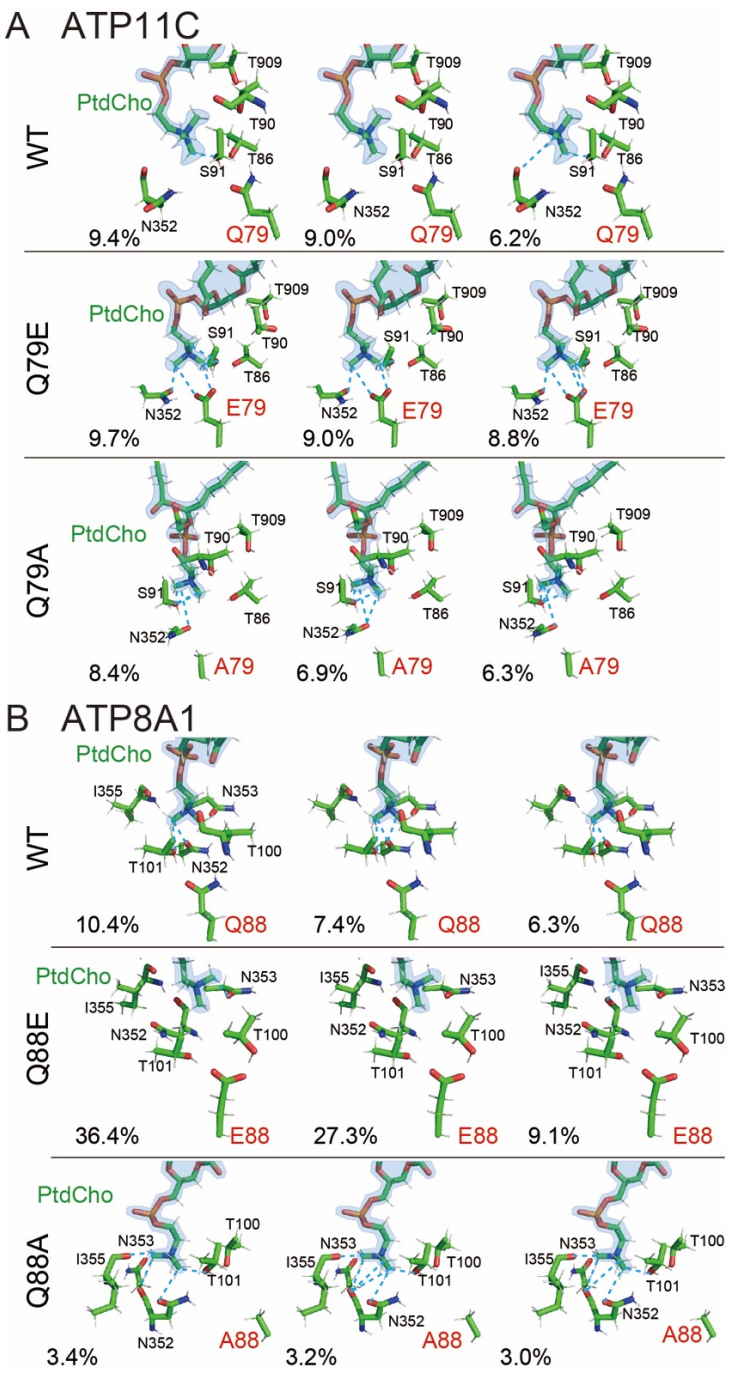

Supplementary Figure 9. H-bond patterns in ATP11C and ATP8A1 with PtdCho. Three major H-bond patterns with PtdCho in the wild-type (WT) and indicated mutant ATP11C (**A**) and ATP8A1 (**B**) are shown. H-bonds are shown in dashed lines. The percentages of the respective patterns are indicated. PtdCho is enclosed by a blue-shadowed area.

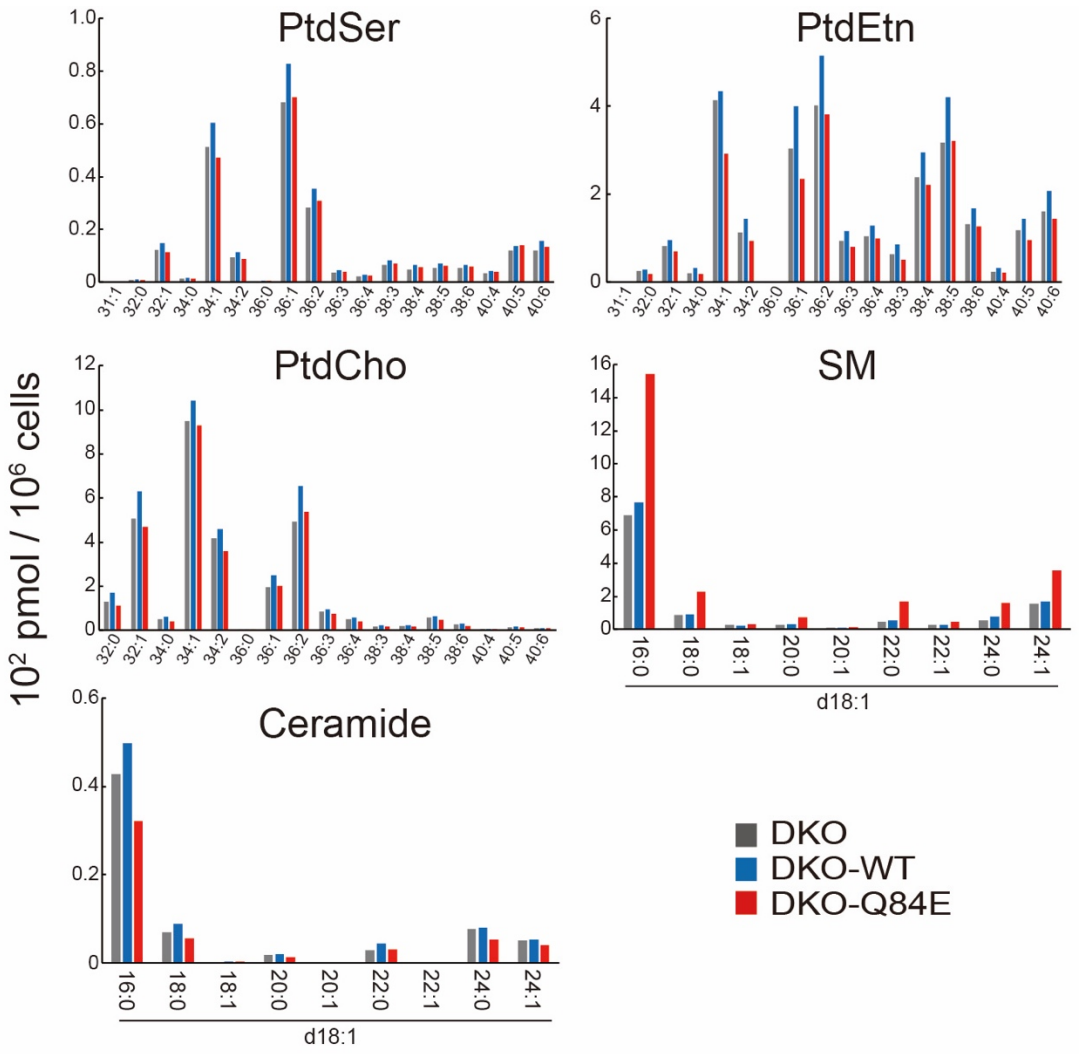

Supplementary Figure 10. LC-MS/MS analysis of cellular lipids. Total lipids were extracted by methanol from DKO or its transformants expressing the WT or Q84E mutant hATP11A (5×10^6 cells) and analyzed by LC-MS/MS together with standard lipids. The amounts of the respective lipids per million cells are shown.

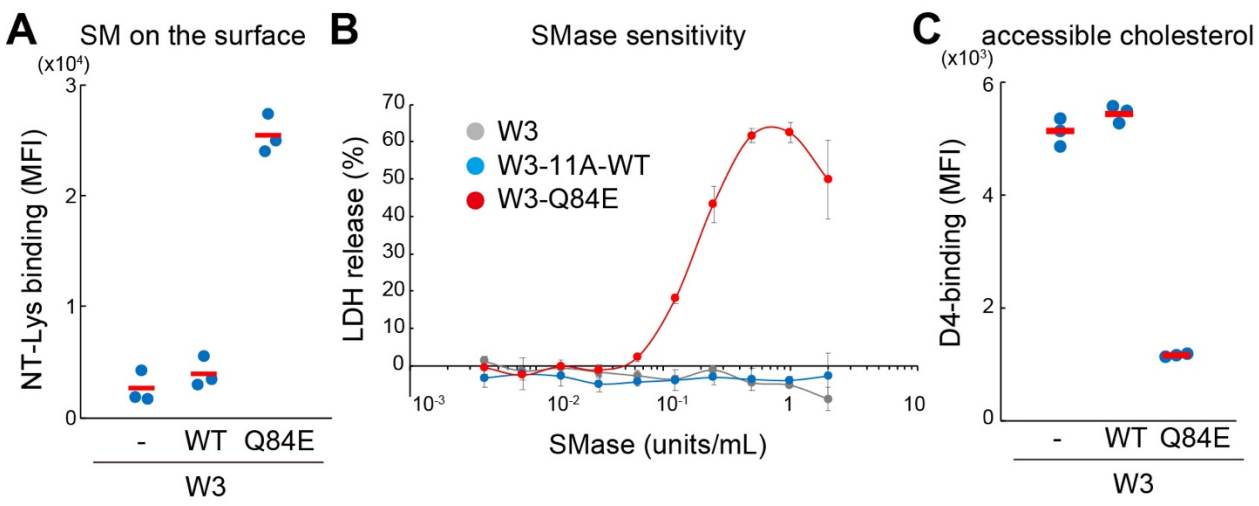

Supplementary Figure 11. An increase in sphingomyelin in the outer leaflet of the plasma membrane in W3 cells expressing the Q84E mutant of hATP11A. W3 cells were transformed with the wild-type or Q84E mutant ATP11A. In (**A**), cells were stained with NT-Lys, analyzed by flow cytometry, and MFI is plotted (n=3). The red bar indicates the average value. In (**B**), cells were incubated with nSMase for 5 minutes, and released LDH was expressed as a percentage of that released with 1% Triton-X100 (n=3). Mean values with S.D. (bar) are shown. In (**C**), cells were stained with mCherry-D4, analyzed by flow cytometry, and MFI is plotted with the average value (bar) (n=3).

Supplementary video 1

An 11-week-old male ATP11A$^{WT/WT}$ littermate as healthy control.

Supplementary video 2

An 11-week-old male ATP11A$^{Q84E/WT}$ mouse. The mouse displayed tremors and an abnormal gait.

Supplementary video 3

A 20-week-old female ATP11A$^{Q84E/WT}$ mouse. The mouse displayed tremors and an abnormal gait.